Turbulent flow and heat transfer enhancement of mixed convection over heated blocks in a channel

Horng-Wen Wu and Shiang-Wuu Perng
Department of System and Naval Mechatronic Engineering, National Cheng Kung University, Tainan, Taiwan, Republic of China

Received November 2002
Revised January 2004
Accepted February 2004

Abstract

Purpose – To investigate the heat transfer enhancement performed by installing a rectangular plate turbulator for internal flow modification induced by vortex shedding.

Design/methodology/approach – The large eddy simulation (LES) and SIMPLE-C method coupled with preconditioned conjugate gradient methods have been applied to the turbulent flow field and heat transfer enhancement of mixed convection in a block-heated channel.

Findings – Provides information about heat transfer performance indicating that heat transfer performance can be affected by various width-to-height ratio of turbulator and Grasehof numbers with a constant Reynolds number. The results show that the installation of turbulator in cross-flow above an upstream block can effectively enhance the heat transfer performance by suitable width-to-height ratio of turbulator and Grasehof numbers.

Research limitations/implications – It is limited to two-dimensional mean flow for the turbulent vortex-shedding flow past a long square cylinder.

Practical implications – A very useful source of information and favorable advice for people developing heat transfer enhancement for electronic devices.

Originality/value – The results of this study may be of interest to engineers attempting to develop thermal control of electronic devices and to researchers interested in the turbulent flow-modification aspects of heat transfer enhancement of mixed convection in a vertical channel.

Keywords Turbulence, Heat transfer, Convection, Numerical analysis

Paper type Research paper

Nomenclature

B = width of the turbulator
C_K = SGS model variable in LES ($C_K = 0.094$)
C_P = pressure coefficient ($\int P\,dA' / \int dA'$)
$[C_P]$ = time-mean pressure coefficient ($\int C_P\,dt / \int dt$)
C_S = Smagorinsky constant
D = hydraulic diameter of channel ($D = 2H$)
dA = surface area increment along the block
dA' = surface area increment along y-axis direction for the turbulator
E_{SGS} = dimensionless subgrid-scale kinetic energy
f_S = frequency of the vortex shedding
f_μ = Van Driest wall damping function ($[1 - \exp(-y_n^+/25)^3]^{1/2}$)
G = grid filter function

The authors gratefully acknowledge the partial financial support of this project by the National Council of the Republic of China.

International Journal for Numerical Methods in Heat & Fluid Flow
Vol. 15 No. 2, 2005
pp. 205-225

0961-5539
DOI 10.1108/09615530510578456

Gr = Grashof number ($g\beta qH^4/k\nu^2$)
h = height of the block, height of the turbulator
H = channel height
l = dimensionless characteristic length scale
L = channel length
n = normal vector
Nu = Nusselt number ($(-1/\theta_w)\,\partial\theta/\partial$n)
[Nu] = time-mean Nusselt number ($\int \mathrm{Nu}\,\mathrm{d}t/\int \mathrm{d}t$)
$\langle$Nu$\rangle$ = surface-mean Nusselt number ($\int \mathrm{Nu}\,\mathrm{d}A/\int \mathrm{d}A$)
P = dimensionless static pressure $\left(P_S/\rho u_\infty^2\right)$
P_S = static pressure
P* = summation of $\overline{P}$ and $\frac{2}{3}E_{SGS}$
Pr = Prandtl number (ν/λ)
Pr_T = turbulent Prandtl number
q = heat flux at wall boundary
R = computational domain
Re = Reynolds number based on channel height ($u_\infty H/\nu$)
Re_D = Reynolds number based on twice channel height ($u_\infty D/\nu$)
Re_{eff} = effective Reynolds number ($1/\mathrm{Re}_{eff} = 1/\mathrm{Re} + 1/\mathrm{Re}_{SGS}$)
Re_{SGS} = SGS Reynolds number ($u_\infty H/\nu_{SGS}$)
St = Strouhal number ($\mathrm{St} = hf_S/u_\infty$)
S_{ij} = strain rate tensor of the flow field $\left(S_{ij} = \frac{1}{2}\left(\frac{\partial u_i}{\partial x_j} + \frac{\partial u_j}{\partial x_i}\right)\right)$
$|\overline{S}|$ = mean strain ($|\overline{S}| = \sqrt{2\overline{S}_{ij}\overline{S}_{ij}}$)
S_Φ = source term for variable
T* = temperature
T_∞ = uniform inlet temperature
t = dimensionless time ($t^*/(H/u_\infty)$)
t* = time
Δt = dimensionless time interval
u, v = dimensionless velocity components ($u = u^*/u_\infty$, $v = v^*/u_\infty$)
u_∞ = uniform inlet velocity
u_τ = friction velocity $\left(u_\tau \equiv \sqrt{\frac{\tau_W}{\rho}}\right)$
u*, v* = velocity components
w = width of the block
x, y = dimensionless x*, y* coordinates ($x = x^*/H$, $y = y^*/H$)
x*, y* = physical coordinates
x_i = Cartesian coordinates ($i = 1$ for x-coordinate; and $i = 2$ for y-coordinate)
y_w = near-wall distance
y_n^+ = dimensionless distance from the wall $\left(y_n^+ \equiv \frac{y_w u_\tau}{\nu}\right)$

Greek symbols
$\overline{\Delta}$ = grid filter width
Φ = general dependent flow variable
Φ' = subgrid-scale component of Φ
Γ_Φ = diffusion coefficient
λ = thermal diffusivity
ν = laminar kinematic viscosity
ν_{SGS} = SGS kinematic viscosity
ρ = density
τ_W = wall shear stress
θ = dimensionless temperature $\left(\left(T^* - T_\infty^*\right)/(qH/k)\right)$
ξ = natural coordinate in computational domain
ζ = dimensionless distance along ribbed wall in Lockett (1987)

Superscript
– = spatial grid filter indication

Subscripts
i,j = indication of components
w = indication of wall boundary

1. Introduction

In recent years, a few researchers have brought up thermal problems for an electronic device (Murakami and Mikic, 2001; Hetsroni *et al.*, 2001) because of having been more compact and densely packaged in response to the demands for cost savings and higher performance. Improvements in cooling methods are required to avoid unacceptable temperature rises. The air-cooling of an array of rectangular sources is of particular interest. Mixed convection has recently received considerable attention because the heat transfer is important within electronic components.

Several studies have been done on the heat transfer enhancement in the forced convection regime by means of vortex generators. Sparrow *et al.* (1983) experimentally investigated the effect of implemented barriers in arrays of rectangular modules and reported significant improvement in the heat transfer coefficient of the module in the second row downstream of the barrier. Myrum *et al.* (1996) performed a series of experiments on dealing vortex generators (circular rods) induced enhancement of heat transfer from ribbed ducts in which different configurations of generators were investigated by changing rod diameter, rod-rib spacing and rod-rod spacing. Chou and Lee (1988) conducted an experimental work on the possibility of reducing flow non-uniformities in LSI packages by vortex generating from a rectangular on the top of a down-stream chip.

Many studies have been conducted on enhancement techniques for forced convection, but there are few studies on natural convection. One of enhancement techniques is to modify flow pattern through vortex-shedding employing little on mixed convection enhancement. Wu and Perng (1998) presented a numerical study on the heat transfer enhancement of laminar flow through vortex shedding from an inclined plate in a heated-blocks channel. The enhancement technique investigated here is to use a rectangular turbulator with various width-to-height ratios to generate vortex shedding in a vertical block-heated channel. Examining the efficacy of the enhancement technique for mixed convection in the turbulent flow is a motivation to us from practical consideration. The present research is a numerical study of mixed convection enhancement in the turbulent flow. The purpose of this study is to quantify the influence of width-to-height ratio of the rectangular turbulator on heat transfer enhancement with various Grashof numbers.

The Reynolds-averaged simulations require a fine grid to resolve the regions of rapid variations. Given the complexity of the Reynolds-averaged simulations, a large eddy simulation (LES) might actually be simpler, shorter in execution and more accurate. In the Reynolds-averaged simulations the length scales of the turbulence usually are much larger than the grid spacing. The Reynolds-averaged simulations only reveal unsteady motions of scales larger than the model's turbulence scale. Besides, the eddy viscosity is obtained from the length scale of the smallest eddy in the turbulent models. Therefore, the volume-average filtered Navier-Stokes equations are fairly insensitive to the turbulent models in a LES (Fureby *et al.*, 1997). Real turbulence is fully three-dimensional, but the turbulent vortex-shedding flow past a long square cylinder, which is two-dimensional in the mean, may be simulated by LES. When the mean flow is two-dimensional, it is common for engineering problems to perform two-dimensional computation, because CPU time is then reduced greatly in comparison with three-dimensional computation (Sakamoto *et al.*, 1993).

In this paper, the SIMPLE-C algorithm (Van Doormaal and Raithby, 1984) is employed to conduct LES task (Galperin and Orszag, 1993) in investigating the fluid modification by means of vortex shedding generated by a rectangular turbulator and its effect on heat transfer enhancement of mixed convection occurring in heated blocks. Second-order backward Euler (SBE) method (Deng *et al.*, 1994) is implemented for the transient term discretizied to remove stability restrictions and extended linear upwind differencing (ELUD) method (Tsui, 1991) (third-order scheme) for the convection terms discretized to avoid severe oscillations. Also, iterative solution methods based on

the preconditioned conjugate gradient method (Kershaw, 1978; Van Der Vorst, 1992) were incorporated into the solving process with second-order time advancement.

The above discretization techniques implemented into the SIMPLE-C algorithm generally requires less computer storage and computation time than the conventional SIMPLE method. The results of this study may be of interest to engineers attempting to develop thermal control of electronic devices and to researchers interested in the turbulent flow-modification aspects of heat transfer enhancement of mixed convection in a vertical channel.

2. Prediction procedure

Turbulent mixed convection heat transfer over heated blocks mounted on one side of the vertical channel is considered in this paper. This two-dimensional flow geometries with and without a turbulator are shown in Figure 1. Calculation of the thermal turbulent flow field in the channel requires obtaining the solution of the governing equations.

In LES the flow variables are decomposed into a large-scale component, denoted by an overbar, and a subgrid-scale (SGS) component. The large-scale component is defined by the following operation:

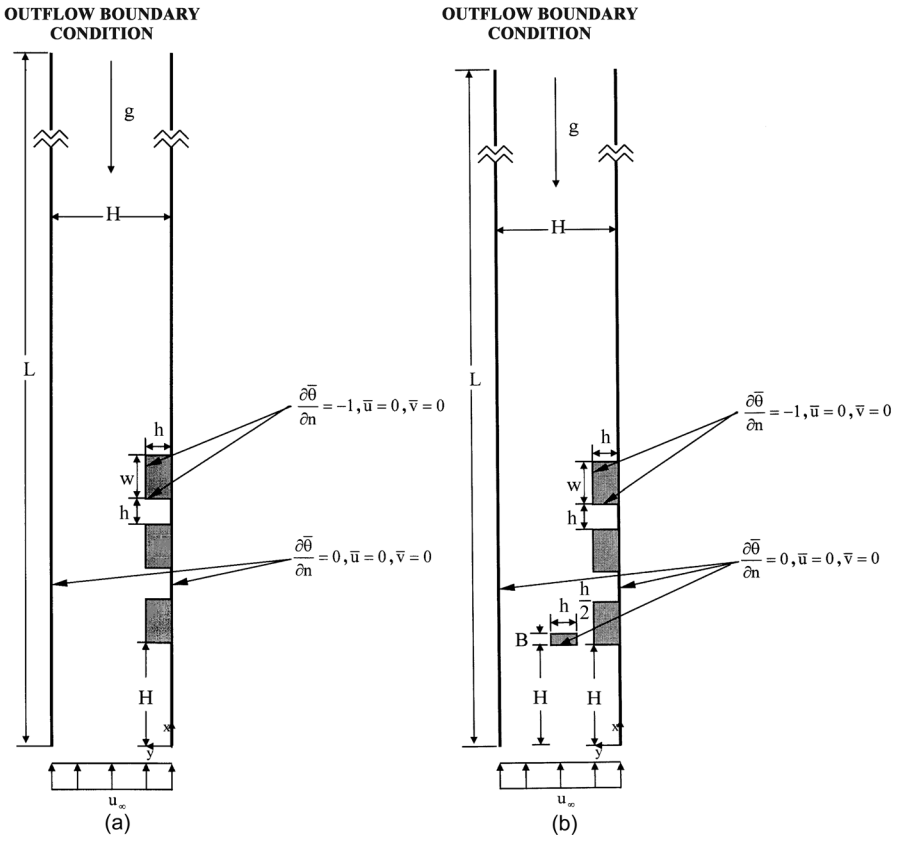

Figure 1.
The geometries considered here: (a) without a rectangular turbulator; and (b) with a rectangular turbulator above the first block

$$\overline{\Phi}(x_i, t) = \int_R G(x_i - \xi)\Phi(\xi)\,\mathrm{d}\xi, \quad \Phi = \overline{\Phi} + \Phi' \tag{1}$$

where the integral is extended over the entire domain R, and G is the grid filter function. The length associated with G is the grid filter width ($\overline{\Delta}$).

The dimensionless transport equations representing the conservation of mass, momentum and thermal energy are cast into a general form of time-dependent and two-dimensional Cartesian coordinates, and the dimensionless governing transport equations filtered by a simple volume-averaged box filter under the Boussinesq approximation (Habchi and Acharya, 1986) are:

$$\frac{\partial\overline{\Phi}}{\partial t} + \frac{\partial}{\partial x}(\bar{u}\overline{\Phi}) + \frac{\partial}{\partial y}(\bar{v}\overline{\Phi}) = \frac{\partial}{\partial x}\left(\Gamma_\Phi \frac{\partial\overline{\Phi}}{\partial x}\right) + \frac{\partial}{\partial y}\left(\Gamma_\Phi \frac{\partial\overline{\Phi}}{\partial y}\right) + S_\Phi(x, y) \tag{2}$$

where $\overline{\Phi}$ represents one of the following entities: 1, u, v, or θ, in which the dependent dimensionless variables are velocity components u, v, and temperature θ. Also, t is dimensionless time, and Γ_Φ and S_Φ stand for the corresponding effective diffusion and source term, respectively. The corresponding expressions of Γ_Φ and S_Φ are given in Table I. In equation (2), the notation $\overline{\Phi} = 1$ denotes the continuity equation.

In Table I, $\mathrm{Re}_{\mathrm{SGS}}$ is the SGS Reynolds number, $\mathrm{Re}_{\mathrm{eff}}$ is the effective Reynolds number, P is the static pressure, and E_{SGS} is the SGS turbulent kinetic energy.

2.1 Turbulence modeling

Initial runs of the present research revealed that the conventional Smagorinsky (1963) model did not generate appropriate levels of eddy viscosity in the complex physical domain. For the reason, the Van Driest wall damping SGS model (Piomelli, 1993) is used here as follows:

$$\frac{1}{\mathrm{Re}_{\mathrm{SGS}}} = l^2 \times \sqrt{2 \times \tilde{S}_{ij}\tilde{S}_{ij}}, \quad l = C_{\mathrm{S}} f_\mu \overline{\Delta}, \quad f_\mu = \left[1 - \exp\left(-y_n^+/25\right)^3\right]^{1/2} \tag{3}$$

where l is a dimensionless characteristic length scale of small eddies, C_{S} is equal to 0.15 (Sakamoto *et al.*, 1993), f_μ is the Van Driest wall damping function, and $y_n^+ \equiv y_{\mathrm{w}} u_\tau / \nu$. The Van Driest wall damping function is used to account for the near wall effect. S_{ij} is a dimensionless strain rate tensor of the filtered flow field.

Φ	Γ_Φ	S_Φ
1	0	0
u	$\frac{1}{\mathrm{Re}_{\mathrm{eff}}}$	$-\frac{\partial P^*}{\partial x} + \frac{\partial}{\partial y}\left(\frac{1}{\mathrm{Re}_{\mathrm{eff}}}\frac{\partial\bar{v}}{\partial x}\right) + \frac{\partial}{\partial x}\left(\frac{1}{\mathrm{Re}_{\mathrm{eff}}}\frac{\partial\bar{u}}{\partial x}\right) + \frac{\mathrm{Gr}}{\mathrm{Re}^2}\bar{\theta}$
v	$\frac{1}{\mathrm{Re}_{\mathrm{eff}}}$	$-\frac{\partial P^*}{\partial y} + \frac{\partial}{\partial y}\left(\frac{1}{\mathrm{Re}_{\mathrm{eff}}}\frac{\partial\bar{v}}{\partial y}\right) + \frac{\partial}{\partial x}\left(\frac{1}{\mathrm{Re}_{\mathrm{eff}}}\frac{\partial\bar{u}}{\partial y}\right)$
θ	$\frac{1}{\mathrm{Pr}\,\mathrm{Re}} + \frac{1}{\mathrm{Pr}_{\mathrm{T}}\,\mathrm{Re}_{\mathrm{SGS}}}$	0

Notes: $\frac{1}{\mathrm{Re}_{\mathrm{eff}}} = \frac{1}{\mathrm{Re}} + \frac{1}{\mathrm{Re}_{\mathrm{SGS}}}$, $P^* = \overline{P} + \frac{2}{3}E_{\mathrm{SGS}}$, $E_{\mathrm{SGS}} = \left(\frac{1}{C_{\mathrm{K}}\overline{\Delta}} \cdot \frac{1}{\mathrm{Re}_{\mathrm{SGS}}}\right)^2$, C_{K}=0.094 (Yoshizawa and Horiuti, 1985), $\mathrm{Pr}_{\mathrm{T}} = 0.9$ (Verman *et al.*, 1992)

Table I.
Definition of Φ, Γ_Φ and S_Φ

$$\overline{S}_{ij} = \frac{1}{2}\left(\frac{\partial \bar{u}_i}{\partial x_j} + \frac{\partial \bar{u}_j}{\partial x_i}\right), \quad |\overline{S}| = (2 \times \overline{S}_{ij}\overline{S}_{ij})^{0.5} \tag{4}$$

2.2 Computational domain, boundary and initial conditions

The geometrical relations for the two channels (Figure 1) are set forth: $H/w = 2.5$, $L/w = 25$, $h/w = 0.5$ and different B/h values (0.25, 0.5 and 1). The streamwise and *cross-stream* directions are x and y, respectively.

Flow and temperature fields in the near-wall region are matched to the boundary layer models. According to the previous study (Werner and Wengle, 1989), we assume that the instantaneous tangential velocity inside the first grid cell is in phase with the instantaneous wall shear stress and that a linear or 1/7 power-law distribution of the instantaneous velocity is assumed:

$$\frac{\bar{u}}{u_\tau} = y_n^+ \quad \left(\text{when } y_n^+ \le 11.81\right) \tag{5}$$

$$\frac{\bar{u}}{u_\tau} = 8.3 y_n^{+1/7} \quad \left(\text{when } y_n^+ > 11.81\right) \tag{6}$$

where u_τ is the friction velocity and y_n^+ is the dimensionless distance from the wall. It should be mentioned that all wall models were basically developed for attached flows and their application in separated flow regions is somewhat questionable. Thermal near-wall boundary conditions coherent with the above instantaneous velocity ones were also implemented. They were based on the universal temperature profiles of Jayatilleke (1969) for a Prandtl number of 0.71.

Besides, we use the following boundary conditions for computations. Cases with and without a rectangular turbulator have the same external boundary conditions; uniform inflow with $\bar{u} = 1$, $\bar{v} = 0$; no-slip boundary conditions $\bar{u} = 0$ and $\bar{v} = 0$ on the upper and lower channel surfaces; and a standard outflow condition $\partial \bar{u}/\partial x = 0$ and $\partial \bar{v}/\partial x = 0$ across the outflow plane, $\partial \bar{\theta}/\partial n = -1$ along the heated block surfaces, and $\partial \bar{\theta}/\partial n = 0$ along the other surfaces. The rectangular turbulator represents a no-slip surface $\bar{u} = 0$ and $\bar{v} = 0$ with zero temperature gradient $\partial \bar{\theta}/\partial n = 0$. The initial conditions are $\bar{u} = \bar{v} = \bar{\theta} = 0$ in the computational domain for $t = 0$. As usual, a physical quantity of great interest is the local Nusselt number Nu along the heated block surfaces. The definition of Nu has been given as

$$\mathrm{Nu} = -\frac{1}{\theta_w}\frac{\partial \theta}{\partial n},$$

where n denoted normal to the heated block surfaces.

2.3 Numerical methods

The SIMPLE-C algorithm with the control volume approach is adopted to derive the discretization of all transport equations arranged into transient, diffusion, convection, and source terms.

2.3.1 Convection term and time advancement. By adopting an ELUD for discretizing the convective terms and a SBE for discretizing the transient term, we may derive

the fully discretized equations by means of control-volume method. These discretized equations are easily implemented into the SIMPLE-C algorithm.

2.3.2 Iterative method. The iterative solution methods based on the preconditioned conjugate gradient method are incorporated into this code. In this paper, the ICCG method (Kershaw, 1978) is used for the Poisson pressure correction equation, and the ILUBiCG method (Van Der Vorst, 1992) is used for u, v and θ equations. The dimensionless time step was tested to be set as 0.001 for the calculations of unsteady flow and heat transfer in the block-mounted channel with and without a turbulator. The calculations were terminated when the mass residual is less than 10^{-4} and the solution for nodal velocity components varied less than 10^{-5} between two consecutive iterations.

3. Results and discussion

3.1 Model validation

A detailed numerical study has been carried out on unsteady turbulent flow and mixed convection heat transfer enhancement by placing a rectangular turbulator in a block-heated channel. In this study, the Grashof number is taken as 0, 2.5×10^7 and 5×10^8 when Reynolds number is kept constant at 5,000 and Prandtl number as 0.71. All the calculations have been performed by using a Pentium III 1G PC. After a series of grid independent test runs (150×40; 220×60; 300×80; 360×100, the former is for x-axis and the latter is for y-axis), the mesh (220×60) was chosen for all cases (the sensitivity results as shown in Figure 2(a)). The time step size is adjusted in this numerical code from stability and accuracy criteria with the initial time step size given as an input by the user. The four time steps 0.0005, 0.001, 0.002, and 0.004 were chosen to test the time step size sensitivity. According to the results shown in Figure 2(b), the time increment Δt was set as 0.001 in the calculations of unsteady turbulent flow and heat transfer over heated blocks with and without a rectangular turbulator. In these calculations for the study, about 14,000 time steps were necessary to obtain reasonably reliable statistics. The computation of CPU times were about 16 h 11 min 27 s for the case without a turbulator and 21 h 18 min 15 s ~ 22 h 8 min 54 s for the cases with a turbulator.

To show that the program in this study can handle turbulent heat transfer and boundary step changes in the channel, we apply the present method to solve the turbulent flow in the ribbed channel employed in the experiments of Lockett (1987). The ratio of square rib height ($h = w$) to channel height (h/H) was 1/9.5, the ratio of channel length to channel height was 8 and $\mathrm{Re_D}$ was 30,000 in the ribbed channel for Lockett's experiment. The periodic boundary condition was imposed along the streamwise direction (x). Besides, the bottom wall has a constant heat flux q on the horizontal wall between the ribs and a value $q/3$ on each face of a rib while the top wall was adiabatic for the thermal boundary conditions in the ribbed channel. The mesh size employed for the comparison with references was 96×48 (along x and y directions, respectively). The steady-state solution is obtained by the numerical procedure as mentioned in the previous section. The present predictions for the normalized Nusselt number $\mathrm{Nu}/\langle \mathrm{Nu} \rangle$ are used to make a comparison with the numerical results calculated by Ciofalo and Collins (1992) and the experimental results measured by Lockett as shown in Figure 3. The comparisons demonstrate that the present method gives better

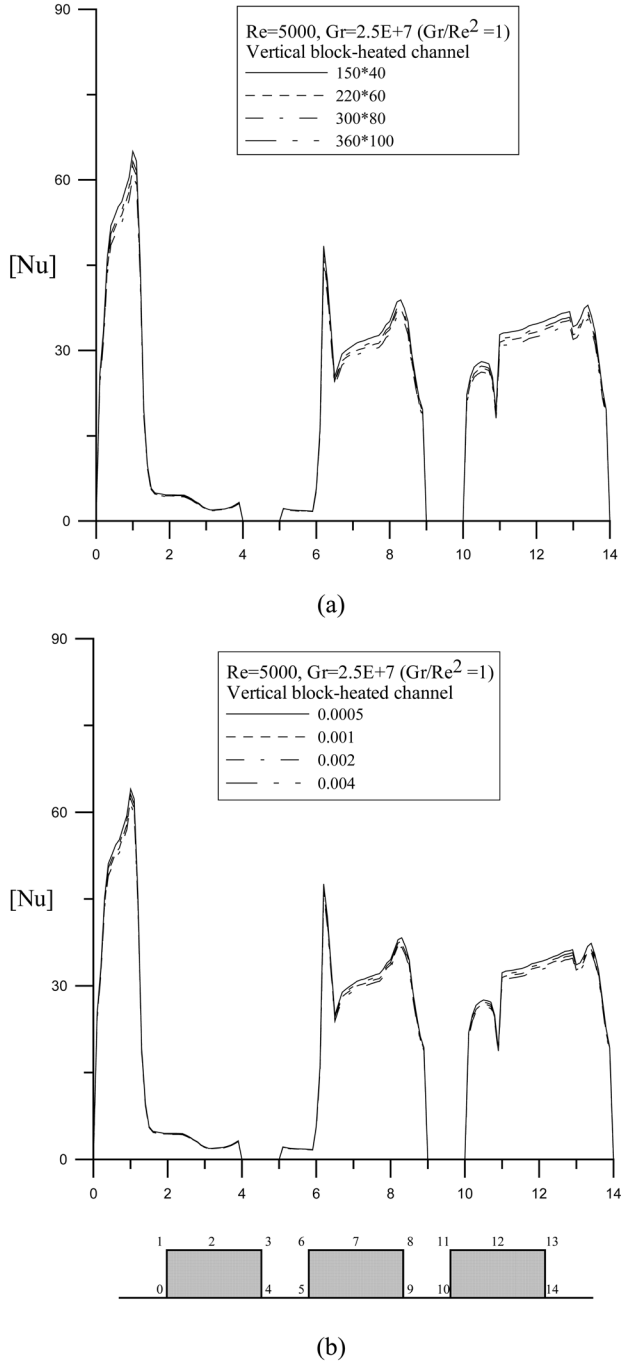

Figure 2.
(a) Grid sensitivity; and (b) time step size sensitivity at $Gr/Re^2 = 1$ and $Re = 5,000$ for no rectangular turbulator in the vertical block-heated channel

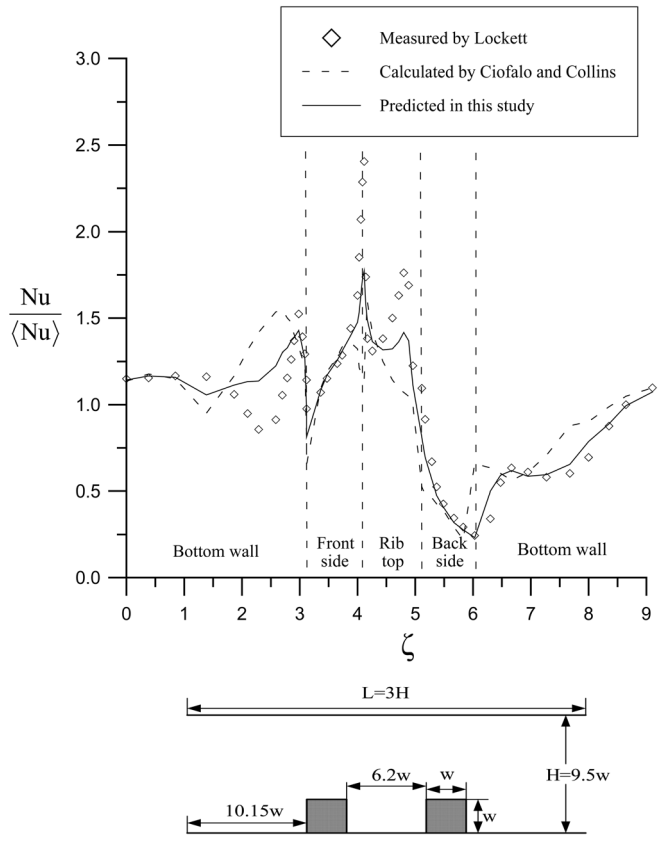

Figure 3.
Comparison between the numerical predictions and Lockett's experimental results

predictions for the normalized Nusselt number than Ciofalo and Collins did, and agrees well with the experimental results of Lockett.

3.2 Influence of buoyancy in the absence of a turbulator

The major effect of buoyancy is to alter the velocity and temperature fields in the forced-convection flow, and this hence alters the Nusselt number. This paper consider the case of upward forced convection over a vertical channel. If the surface is heated so that wall temperature is larger than the inlet temperature, the resulting buoyancy force aids the convection motion, especially in the near-wall region, and we would expect the Nusselt number to be greater than the forced-convection value at that Reynolds number (Kays and Crawford, 1993). Time-mean Nusselt number will be used below for comparing the turbulent heat transfer characteristics between the case with a rectangular turbulator and the case without a turbulator. The time-mean Nusselt number for heated blocks with a rectangular turbulator is calculated in time interval containing several flow cycles of vortex shedding, while the time-mean Nusselt number for the case without a turbulator is calculated in the same time interval. In Figure 4, the local Nusselt number shows that the same characteristic behavior increases with an

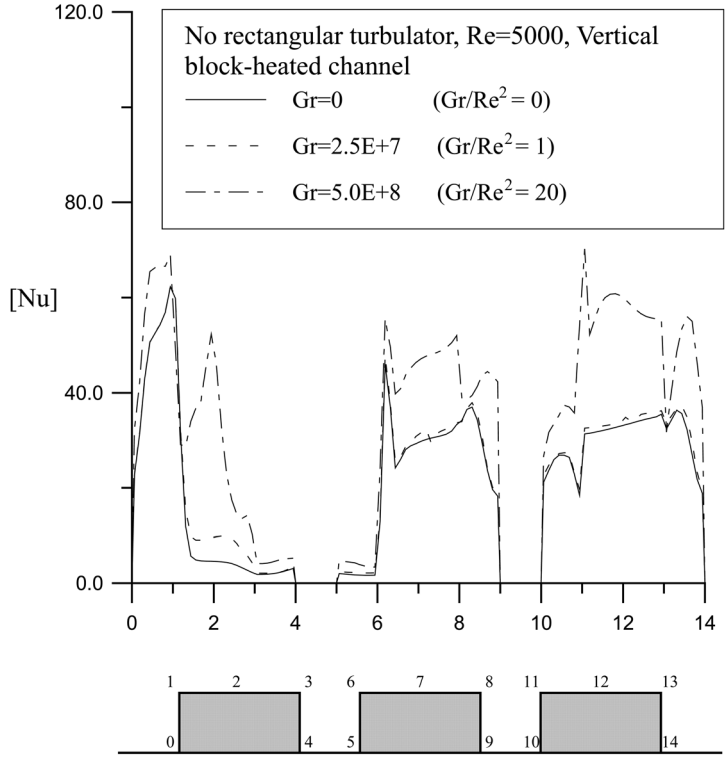

Figure 4.
Time-mean Nusselt number profiles along the block surfaces for Gr/Re^2 values at $Re = 5,000$

increase in the Gr/Re^2 value. The maximum local Nusselt number for a given block occurs at the front corner while the minimum value occurs at the groove between two blocks. The influence of mixed convection is prominent, especially along the horizontal surfaces of the blocks (in the x direction). Similar influence has been presented in an earlier study (Kim *et al.*, 1992). For understanding the profiles of Nusselt number further, the streamlines for various Gr values ($Gr = 0$, 2.5×10^7, 5×10^8) shown in Figure 5 was utilized to explain these results. The fluid flow around the blocks placed on the lower wall of a channel is very complicated since it is defined by stagnation in front of the first block, separation at the front corner of the first block, a recirculation in the groove between two blocks and another recirculating zone behind the third block (Figure 5). The curvature of the streamline becomes very large locally at the front corner of a given block; this has a high velocity, so the convection heat transfer is large. Because of separation in front of the first block, there is a small standing vortex around the lower wall of channel. Besides, this standing vortex is becoming smaller and far away from the front side of the first block when the Gr/Re^2 value becomes large. A recirculating zone is formed in the groove between two blocks, so that the heat is transferred poorly from the groove fluid to the mainstream flow. Figure 5 also shows that there are a bigger clockwise vortex and a smaller counterclockwise vortex in the recirculating zone behind the last block; the recirculating zone is becoming smaller when the Gr/Re^2 values becomes large. Besides, the recirculating zone above the roof

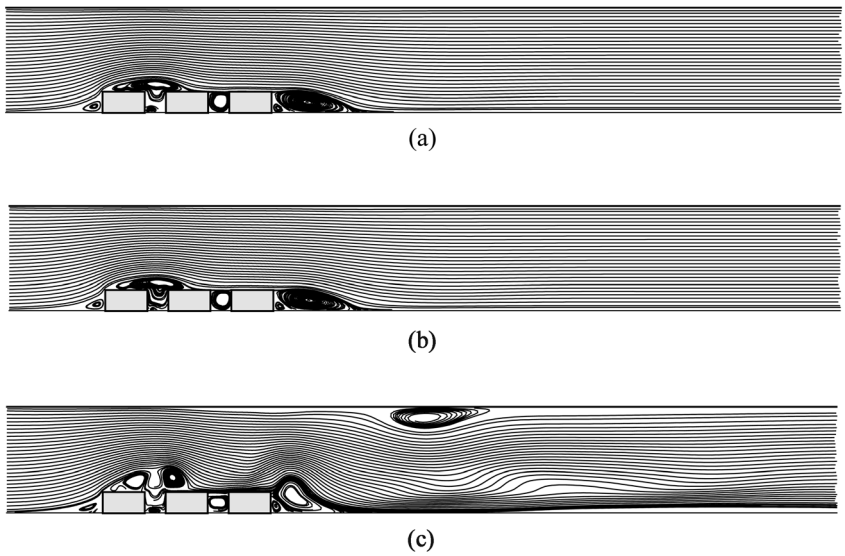

Figure 5.
Stream patterns for $Re = 5,000$ at $t = 30$: (a) $Gr/Re^2 = 0$; (b) $Gr/Re^2 = 1$; and (c) $Gr/Re^2 = 20$

around the first two blocks is divided into two smaller recirculations and another recirculation is formed around the upper wall of channel when the Gr/Re^2 value is equal to 20. This recirculating zone above the roof around the first two blocks makes the heat transfer poor from the horizontal surfaces of the heated block to the mainstream flow, so the distribution of Nusselt number along the surfaces on the roof is obviously smaller than other surfaces shown in Figure 4. This can be explained by noting that the buoyancy effect causes the streamlines to be uplifted from the horizontal surfaces of the blocks. Consequently, the dividing streamline, which separates the recirculating zone, has to travel shorter distances in comparison with the case of a purely forced convective flow. The result of Figure 5 can provide confirmation to the flow processes.

3.3 Influence of buoyancy in the presence of a turbulator

The heat transfer enhancement of a rectangular turbulator installed above the first block is shown in Figure 6 for three different Gr/Re^2 values at $Re = 5,000$. The profile of time-mean Nusselt number along the surfaces of heated blocks increases in comparison with the case without a turbulator as shown in Figure 4. The flow fields shown in Figure 7 can explain this result. Figure 7 shows the flow fields for the corresponding instantaneous stream patterns each time at the minimum value of pressure coefficient C_P in one vortex-shedding cycle. When $Gr/Re^2 < O(1)$ (Figure 7(a) and (b)), wave flows behind the rectangular turbulator pass stronger and faster across these heated blocks, then weaker and slower behind the third block. The wave motion changes the flow field behind the last block from one recirculating zone into two recirculating zones; the one close to the side surface of the last block is small, and the other one is large. At $Gr/Re^2 = 20$ (Figure 7(c)) the buoyancy upflow along the horizontal surfaces of the blocks may strengthen the wave flows behind the turbulator. Besides, the smaller recirculating zone behind the last block becomes larger and closer

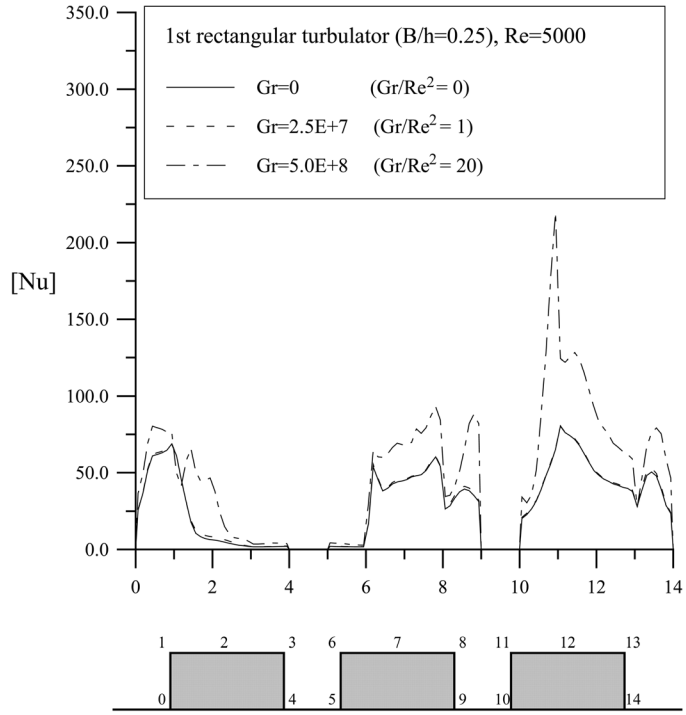

Figure 6.
Effect of Gr/Re^2 values on time-mean Nusselt number profiles installing a rectangular turbulator ($B/h = 0.25$) at $Re = 5,000$

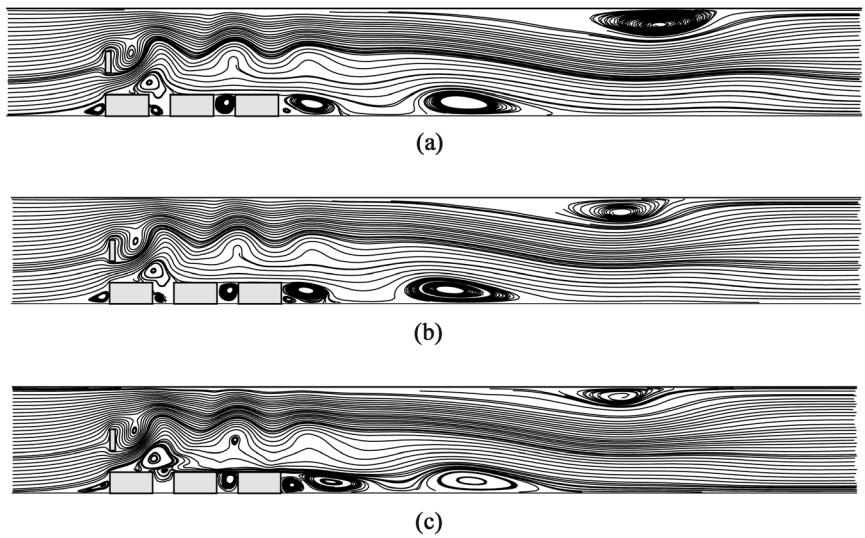

Figure 7.
Stream patterns installing a rectangular turbulator ($B/h = 0.25$) for $Re = 5,000$:
(a) $Gr/Re^2 = 0$;
(b) $Gr/Re^2 = 1$; and
(c) $Gr/Re^2 = 20$

to the other recirculating zone because the strong buoyancy effect uplifts the streamlines from the horizontal surface of the last block. On the whole, the wave flows can improve the heat transfer along the blocks as shown in Figure 6.

3.4 Influence of the turbulator geometry

For various B/h values the installation of the rectangular turbulator increases the distribution of time-mean Nusselt number along the block surfaces (Figure 8). For various B/h values the instantaneous streamlines at the corresponding flow condition are shown in Figure 9 each time at the minimum of pressure coefficient C_P in one vortex-shedding cycle. For the turbulator with various B/h values, it is evident from Figure 9 that the separated flow goes along the surfaces and always reattaches on either the upper or the lower surface during a period of the vortex shedding into the wake. Besides, the use of the rectangular turbulator locally accelerates fluid flow through the passageway between the turbulator and the first block, but produces different patterns of wave motion induced by vortex shedding. The oscillating fluid motion generated by the turbulator can effectively assist heat transfer along the block surfaces. The improvement in heat transfer for $Gr/Re^2 < O(1)$ is mainly caused by the oscillations generated by the turbulator. When $Gr/Re^2 > O(1)$, the heat transfer is improved mainly by a result of the oscillations forcing the mainstream flow to mix with the buoyant upflow along the horizontal surfaces of the heated blocks. In Figure 9,

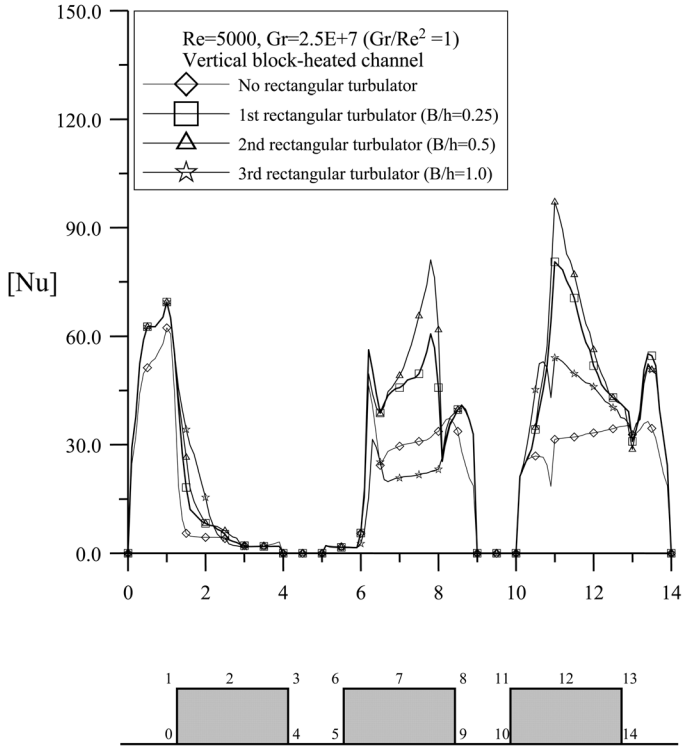

Figure 8.
Influence of width-to-height ratios (B/h) on time-mean Nusselt number profiles compared to no turbulator at $Gr = 2.5 \times 10^7$ and $Re = 5,000$

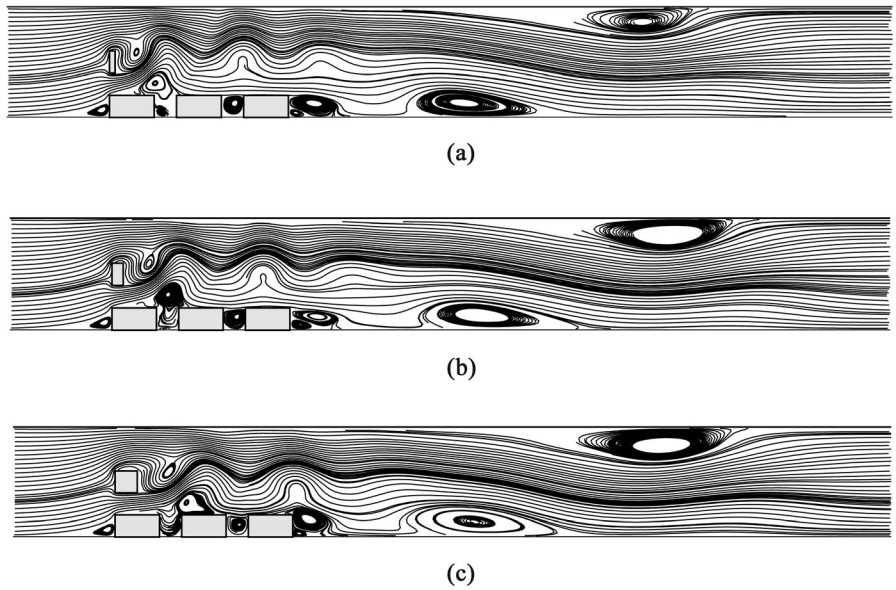

Figure 9.
Stream patterns for various width-to-height ratios at $Gr = 2.5 \times 10^7$ and $Re = 5,000$: (a) $B/h = 0.25$; (b) $B/h = 0.5$; and (c) $B/h = 1$

the recirculation above the roof of the first two blocks is moving downstream when the ratio B/h becomes large. The heat is hence transferred poorly from the horizontal surfaces of these two heated blocks to the mainstream flow. These results are used to explain that the time-mean Nusselt number is smaller along the horizontal surface of the second block with a turbulator ($B/h = 1$) than without a turbulator.

The time variations of the flow patterns installing a rectangular turbulator ($B/h = 0.25$) during the flow cycle for $Gr = 2.5 \times 10^7$ and 5.0×10^8 at $Re = 5000$ are shown in Figures 10 and 11, respectively. These two figures cover, respectively, one period of the vortex-shedding process from dimensionless time 12.051-13.303 and 12.038-13.252. This process demonstrates the event that commences with the shedding of a vortex from the leading tip and ends with the shedding of the next vortex from the same point. For $Gr = 2.5 \times 10^7$ and 5.0×10^8, the oscillatory nature of the wake behind the turbulator is similar, but the wave motion for $Gr = 5.0 \times 10^8$ is stronger than for $Gr = 2.5 \times 10^7$. This motion makes a different pattern of the recirculating zone behind the last heated block. Besides, the standing vortex in front of the first block is more slender for $Gr = 5.0 \times 10^8$ than for $Gr = 2.5 \times 10^7$. Figure 12 shows the variation of the pressure coefficient C_P for the rectangular turbulator with $B/h = 0.25$. The Strouhal number is defined by

$$St = hf_S/u_\infty \tag{7}$$

$St = 0.1597$ for $Re = 5,000$ and $Gr = 2.5 \times 10^7$, and $St = 0.1581$ for $Re = 5,000$ and $Gr = 5.0 \times 10^8$. For investigating the influence of buoyancy effect and width-to-height ratio (B/h) of rectangular turbulator on the pressure coefficient C_P and Strouhal number St, the variation of $[C_P]$ and St are, respectively, shown in Figure 13 and Table II. In Figure 13(a), $[C_P]$ is almost the same for different Gr/Re^2 values, in other words, the buoyancy effect on the pressure coefficient C_P is not obvious. Form the profiles of $[C_P]$

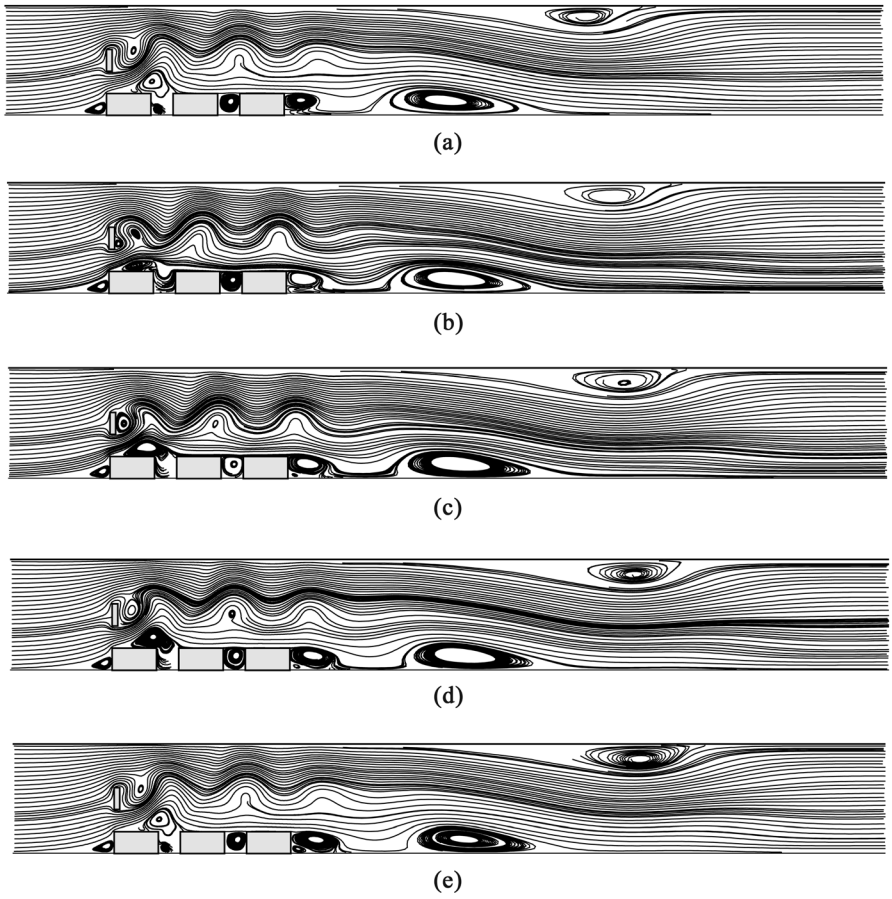

Figure 10.
Sequence of streamlines with a rectangular turbulator ($B/h = 0.25$) during one cycle at: (a) $t = 12.051$; (b) $t = 12.658$; (c) $t = 12.916$; (d) $t = 13.123$; and (e) $t = 13.303$ for $Gr/Re^2 = 1$ and $Re = 5,000$

shown in Figure 13(b), the pressure coefficient decreases with increasing the width-to-height ratio (B/h) for the rectangular turbulator. Besides, increasing the B/h value will delay the vortex-shedding process and make the phase shift of the vortex shedding. In Table II, Strouhal number St, is almost the same for various Gr values while St decreases slowly with increasing the width-to-height ratio (B/h). On the other hand, Strouhal number listed in Table II is from 0.1211 to 0.1598 for all cases. Similar observations have been seen in an earlier study conducted by Okajima (1982).

We can quantify the effect of width-to-height ratio of the rectangular turbulator on the heat transfer enhancement by means of the values of average time-mean Nusselt number for the blocks as follows. The average time-mean Nusselt number is calculated by the values of time-mean Nusselt number on all grid points of the block boundary. The values of average time-mean Nusselt number for the blocks are listed in Table III for various B/h values of the turbulator as well as for no turbulator as the Gr/Re^2 value changes at a fixed value of Re (=5,000). The value of average time-mean Nusselt

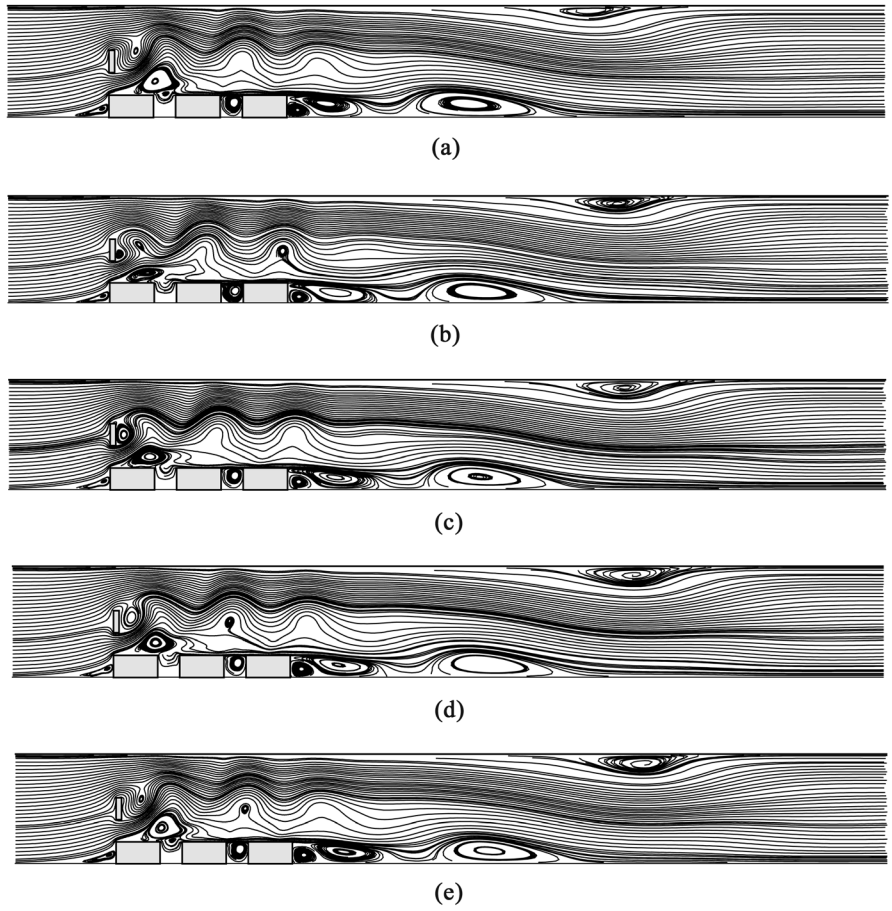

Figure 11.
Sequence of streamlines with a rectangular turbulator ($B/h = 0.25$) during one cycle at: (a) $t = 12.038$; (b) $t = 12.574$; (c) $t = 12.978$; (d) $t = 13.045$; and (e) $t = 13.252$ for $\mathrm{Gr}/\mathrm{Re}^2 = 20$ and $\mathrm{Re} = 5,000$

number for the block increases with increasing Gr for the turbulator as well as for no turbulator. The maximum value of average time-mean Nusselt number exists at the third block, and the value increases progressively from the first block to the third block. The value of average time-mean Nusselt number for the whole block increases with installation of the turbulator compared to no turbulator. The maximum value of average time-mean Nusselt number for the whole block appears at the width-to-height ratio $B/h = 0.5$ with $\mathrm{Gr}/\mathrm{Re}^2 = 20$. As also shown in parentheses in Table III, the maximum increase in time-mean overall average Nusselt number is 55.2 percent at $B/h = 0.5$ with $\mathrm{Gr}/\mathrm{Re}^2 = 0$ because of the small time-mean overall average value for no turbulator. For all cases, the maximum increase in overall average Nu is at $B/h = 0.5$ and the minimum increase is at $B/h = 1.0$; this result is mainly caused by the oscillating wave motion. The wave motion improves the heat transfer best for $B/h = 0.5$ and the minimum improvement for $B/h = 1.0$ because the recirculation around the roof between the first and the second block for $B/h = 0.5$ has less influence

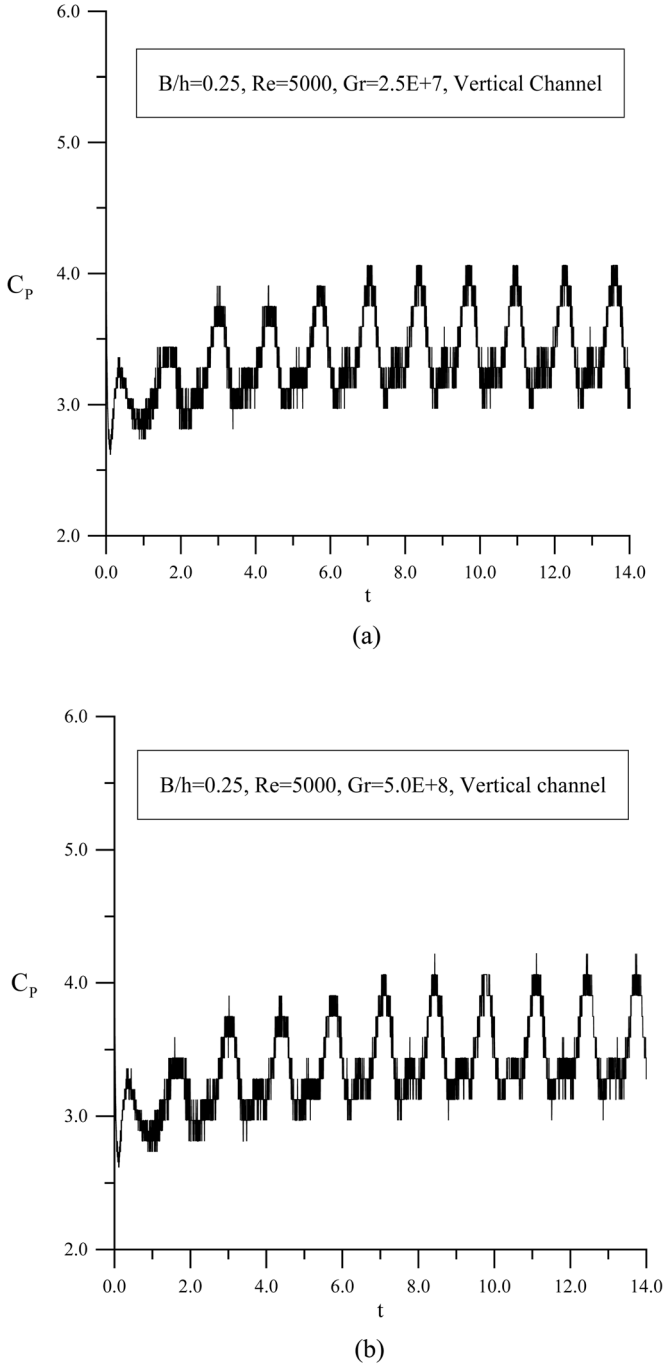

Figure 12.
Pressure coefficient C_P versus dimensionless time for $Re = 5,000$ at: (a) $Gr = 2.5 \times 10^7$ and (b) $Gr = 5.0 \times 10^8$

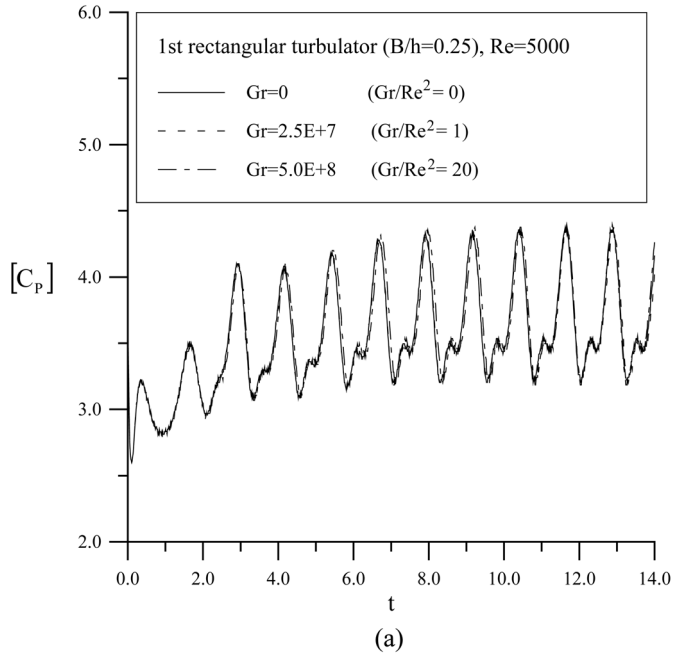

Figure 13.
Influence of various:
(a) Gr/Re^2; and
(b) width-to-height (B/h) values on the time-mean pressure coefficient [C_P] at $Re = 5,000$

on the horizontal surfaces of the first and the second blocks; in contrast, the case for $B/h = 1.0$ has obvious influence on the horizontal surface of the second block. The influence of this recirculation mentioned also in Figure 9 makes the heat transfer poor from the horizontal surface of the block to the mainstream flow.

4. Conclusions

A numerical analysis has been systematically performed for the unsteady turbulent flow and mixed convection heat transfer in a vertical block-heated channel with and without installing a rectangular turbulator above an upstream block. The main conclusions emerging from the results and discussion may be summarized as follows.

(1) The results for normalized Nusselt number computed in this paper are in good agreement with available measurements of Lockett.

(2) Installing a rectangular turbulator can effectively improve the turbulent heat transfer characteristics through the modification of the flow pattern.

(3) For $Gr/Re^2 < O(1)$, the buoyancy effect on the turbulent flow and the heat transfer can be neglected. The wave flows induced by vortex shedding behind the rectangular turbulator pass stronger and faster across these three blocks, then weaker and slower behind the last block.

(4) When $Gr/Re^2 = 20$, the buoyancy effect obviously exists along the horizontal surfaces of the blocks. The strong buoyant upflow along the horizontal surfaces

Table II. Strouhal number, St, for various B/h and Gr/Re^2 values at $Re = 5,000$

	$B/h = 0.25$	$B/h = 0.5$	$B/h = 1.0$
$Gr/Re^2 = 0$ at $Re = 5,000$	0.1598	0.1478	0.1238
$Gr/Re^2 = 1$ at $Re = 5,000$	0.1597	0.1476	0.1236
$Gr/Re^2 = 20$ at $Re = 5,000$	0.1581	0.1462	0.1211

Table III. For three Gr/Re^2 values at $Re = 5,000$, values of average time-mean Nusselt number along the block without and with a rectangular turbulator

Block	No turbulator	$B/h = 0.25$	$B/h = 0.5$	$B/h = 1.0$
$Gr/Re^2 = 0$ at $Re = 5,000$				
1st	17.1461	21.6223 (26.1 percent)	22.4198 (30.8 percent)	23.9091 (39.4 percent)
2nd	22.7416	32.5779 (43.3 percent)	36.0365 (58.8 percent)	19.4950 (− 14.3 percent)
3rd	30.0689	47.5014 (58.0 percent)	50.1040 (66.6 percent)	42.8682 (42.6 percent)
Overall	23.3189	33.9005 (45.4 percent)	36.1868 (55.2 percent)	28.7574 (23.3 percent)
$Gr/Re^2 = 1.0$ at $Re = 5,000$				
1st	19.1353	23.6116 (23.4 percent)	24.4091 (27.6 percent)	25.8983 (35.3 percent)
2nd	23.4897	33.3261 (41.9 percent)	36.7846 (56.6 percent)	20.2432 (− 13.8 percent)
3rd	31.0938	48.5263 (56.1 percent)	51.1289 (64.4 percent)	43.8931 (41.2 percent)
Overall	24.5730	35.1546 (43.1 percent)	37.4409 (52.4 percent)	30.0115 (22.1 percent)
$Gr/Re^2 = 20.0$ at $Re = 5,000$				
1st	30.8604	32.9917 (6.9 percent)	33.7892 (9.5 percent)	35.2784 (14.3 percent)
2nd	34.4102	39.8783 (15.9 percent)	43.3369 (25.9 percent)	26.7955 (− 22.1 percent)
3rd	49.7702	61.5998 (23.8 percent)	64.2024 (29.0 percent)	56.9666 (14.5 percent)
Overall	38.3469	44.8233 (16.9 percent)	47.1095 (22.9 percent)	39.6801 (3.5 percent)

Note: Values in parentheses designating the percentage change relative to no rectangular turbulator

of the blocks interacts with the wave flows and strengthens these flows across the blocks.

(5) The value of time-mean overall average Nusselt number along the blocks increases with increasing the width-to-height ratio of the turbulator except for the width-to-height ratio equal to 1.

References

Chou, J.H. and Lee, J. (1988), "Reducing flow non-uniformities in LSI packages by vortex generator", in Aung, W. (Ed.), *Cooling Technology for Electronic Equipment*, Hemisphere Publishing Corporation, New York, NY, pp. 113-24.

Ciofalo, M. and Collins, M.W. (1992), "Large-eddy simulation of turbulent flow and heat transfer in plane and rib-roughened channels", *Int. J. Num. Methods in Fluids*, Vol. 15, pp. 453-89.

Deng, G.B., Piquet, J., Queutey, P. and Visonneau, M. (1994), "A new fully coupled solution of the Navier Stokes equations", *Int. J. Num. Methods in Fluids*, Vol. 19, pp. 605-39.

Fureby, C., Tabor, G., Weller, H.G. and Gosman, A.D. (1997), "A comparative study of subgrid scale models in homogeneous isotropic turbulence", *Phys. Fluids*, Vol. 9 No. 5, pp. 1416-29.

Galperin, B. and Orszag, S. (1993), *Large Eddy Simulation of Complex Engineering and Geophysical Flows*, Cambridge University Press, Cambridge, pp. 231-346.

Habchi, S. and Acharya, S. (1986), "Laminar mixed convection in a partially blocked vertical channel", *Int. J. Heat Mass Transfer*, Vol. 29, pp. 1711-22.

Hetsroni, G., Mosyak, A. and Segal, Z. (2001), "Nonuniform temperature distribution in electronic devices cooled by flow in parallel microchannels", *IEEE Transactions on Components and Packaging Technologies*, Vol. 24 No. 1, pp. 16-23.

Jayatilleke, C.L.V. (1969), "The influence of Prandtl number and surface roughness on the resistance of the laminar sublayer to momentum and heat transfer", *Prog. Heat Mass Transfer*, Vol. 1, pp. 193-329.

Kays, W.M. and Crawford, M.E. (1993), *Convective Heat and Mass Transfer*, McGraw-Hill, New York, NY.

Kershaw, D. (1978), "The incomplete Cholesky-conjugate gradient method for the iterative solution of systems of linear equations", *J. Comp. Phys.*, Vol. 26, pp. 43-65.

Kim, S.Y., Sung, H.J. and Hyun, J.M. (1992), "Mixed convection from multiple-layered boards with cross-streamwise periodic boundary conditions", *Int. J. Heat Mass Transfer*, Vol. 35 No. 11, pp. 2941-52.

Lockett, J.F. (1987), "Heat transfer from roughened surfaces using laser interferometers", PhD thesis, Department of Mechanical Engineering, The City University, London.

Murakami, Y. and Mikic, B.B. (2001), "Parametric optimization of multichanneled heat sinks for VLSI chip cooling", *IEEE Transactions on Components and Packaging Technologies*, Vol. 24 No. 1, pp. 2-9.

Myrum, T., Acharya, S., Sinha, S. and Qiu, X. (1996), "Flow and heat transfer in a ribbed duct with vortex generators", *ASME Journal of Heat Transfer*, Vol. 118, pp. 294-300.

Okajima, A. (1982), "Strouhal numbers of rectangular cylinders", *J. Fluid Mech.*, Vol. 123, pp. 379-98.

Piomelli, U. (1993), "High Reynolds number calculations using the dynamic subgrid scale stress model", *Phys. Fluids A*, Vol. 5 No. 6, pp. 1484-90.

Sakamoto, S., Murakami, S. and Mochida, A. (1993), "Numerical study on flow past 2D square cylinder by large eddy simulation: comparison between 2D and 3D computations", *Journal of Wind Engineering and Industrial Aerodynamics*, Vol. 50, pp. 61-8.

Smagorinsky, J. (1963), "General circulation experiments with the primitive equations", *Mon. Wea. Rev.*, Vol. 91, pp. 99-164.

Sparrow, E.M., Vemuri, S.B. and Kadle, D.S. (1983), "Enhanced and local heat transfer, pressure drop, and flow visualization", *Int. J. Heat Mass Transfer*, Vol. 26, pp. 689-99.

Tsui, Y.Y. (1991), "A study of upstream weighted high-order differencing for approximation to flow convection", *Int. J. Num. Methods in Fluids*, Vol. 13, pp. 167-99.

Van der Vorst, H. (1992), "BI-CGSTAB: a fast and smoothly converging variant of BI-CG for the solution of nonsymmetric linear system", *SIAM J. Sci. Stat. Comput.*, Vol. 13 No. 2, pp. 631-44.

Van Doormaal, J.P. and Raithby, G.D. (1984), "Enhancements of the SIMPLE method for predicting incompressible fluid flows", *Num. Heat Trans.*, Vol. 7, pp. 147-63.

Verman, A.W., Geurts, B.J., Kuerten, J.G.M. and Zandbergen, P.J. (1992), "A finite volume approach to large eddy simulation of compressible, homogeneous isotropic, decaying turbulence", *Int. J. Num. Methods in Fluids*, Vol. 15, pp. 799-816.

Werner, H. and Wengle, H. (1989), "Large-eddy simulation of the flow over a square rib in a channel", *Proc. 7th Symp. Turbulent Shear Flows*, Stanford University, pp. 10.2.1-6.

Wu, H.W. and Perng, S.W. (1998), "Heat transfer augmentation of mixed convection through vortex shedding from an inclined plate in a vertical channel containing heated blocks", *Num. Heat Trans. Part A*, Vol. 33 No. 2, pp. 225-44.

Yoshizawa, A. and Horiuti, K. (1985), "Statistically-derived subgrid-scale kinetic energy model for the large-eddy simulation of turbulent flows", *Journal of the Physical Society of Japan*, Vol. 54 No. 8, pp. 2834-9.